

NJC

Accepted Manuscript



This is an *Accepted Manuscript*, which has been through the Royal Society of Chemistry peer review process and has been accepted for publication.

Accepted Manuscripts are published online shortly after acceptance, before technical editing, formatting and proof reading. Using this free service, authors can make their results available to the community, in citable form, before we publish the edited article. We will replace this *Accepted Manuscript* with the edited and formatted *Advance Article* as soon as it is available.

You can find more information about *Accepted Manuscripts* in the [Information for Authors](#).

Please note that technical editing may introduce minor changes to the text and/or graphics, which may alter content. The journal's standard [Terms & Conditions](#) and the [Ethical guidelines](#) still apply. In no event shall the Royal Society of Chemistry be held responsible for any errors or omissions in this *Accepted Manuscript* or any consequences arising from the use of any information it contains.



www.rsc.org/njc



27x16mm (300 x 300 DPI)

Copper loaded onto the polymeric magnetic nanocatalyst a retrievable and robust heterogeneous catalyst for click reaction

Ali Pourjavadi*^a, Mahmood Tajbakhsh,^{b*} Maryam Farhang,^b Seyed Hassan Hosseini,^a

^a *Polymer Research Laboratory, Department of Chemistry, Sharif University of Technology, Tehran, Iran*

^b *Organic Chemistry Laboratory, Faculty of Chemistry, University of Mazandaran, Babolsar, 47415, Iran*

E-mail address: Tajbakhsh@ac.ir; Phone/fax: (982)166165311

E-mail address: purjavad@sharif.edu; Phone/fax: (982)166165311

Abstract

A novel heterogeneous copper catalyst based on poly(ionic liquid) coated magnetic nanoparticle was prepared by polymerization of 3-carboxymethyl-1-vinylimidazolium in the presence of surface modified magnetic nanoparticles, followed by coordination of the carboxylate units in the polymer chains with copper sulfate. The resulting catalyst has been high loading level of copper ions and is used in low weight percent. The catalytic activity of the newly designed catalyst was tested in one-pot synthesis of 1,4-disubstituted 1,2,3-triazoles by click reaction between primary halides or tosylates, sodium azide and terminal acetylenes at room temperature in aqueous media. The unique nanocatalyst structure and the multi-layered form of coated polymer on the magnetite surface are responsible for the excellent catalyst performances in click reaction.

Keywords: Magnetic catalyst, Polymer coated magnetic nanoparticles, Poly(ionic liquid), 1,2,3-Triazoles

1. Introduction

The challenging task in chemistry is to develop practical methods, reaction media, conditions, and the use of materials based upon the principles of green chemistry. The concept of “Green Chemistry” has emerged as one of the guiding principles of environmentally benign synthesis [1]. The use of aqueous media in transition-metal catalyzed reactions have become popular [2] because water is non-toxic, non-flammable and easily available and water-based synthetic processes are inherently safer as well as being inexpensive. Moreover, the products can be separated easily by extraction.

1,2,3-Triazole derivatives are an important class of organic compounds for medicinal chemistry, which exhibit a wide range of biological properties such as antiepileptic, anti-allergic [3], anticancer and anti HIV [4]. In general, these compounds are prepared through Huisgen dipolar cycloaddition of organic azides and alkynes [5]. However, because of the high activation energy (ca. 24 - 26 kcal/mol), these cyclo-additions are often very slow even at elevated temperature (80 -120 °C for 12-24 h) and produce mixtures of regioisomers.

The introduction of Cu (I) salts by Sharpless et al. lead to a major improvement in both rate and regioselectivity of the reaction [6]. On the other hand, copper salts as homogeneous catalysis suffer from many problems such as difficult separation and recycling the catalyst, cytotoxicity and environmental pollution. The removal of trace amounts of catalyst from the final product is essential since metal contamination is highly regulated, particularly in the pharmaceutical industry. Even with the extensive methods, elimination of trace amounts of catalyst is a challenge [7].

Immobilization of the homogenous catalysts on solid materials can mitigate these problems. Recently, several methods have been developed to immobilize copper species on a large variety of solid supports. The major problem with using heterogeneous catalysts could be due to low loading of homogeneous catalyst onto the solid bed. In the normal grafting of organic compound onto the solid substrate usually, one layer of organic compound is coated on the surface. Therefore, a large amount of solid catalysts are used for the catalyzing process. On the other hand, use of a large amount of heterogeneous catalysts causes more pollution of the reaction medium, and requires more solvent for the separation process, and recovery of catalyst [8-18]. Among the various supports; Fe₃O₄ nanoparticles can facilitate convenient method for removing and recycling magnetized catalyst from the solution system without the need for any filtration or centrifugation process [19]. The use of magnetic nanoparticles (MNPs) has appeared as an ideal solution to the above stated problems [20- 23].

In this paper, we report the preparation and characterization of a novel heterogeneous copper catalyst based on Fe₃O₄ nanoparticles coated by multi layers of poly functionalized vinyl imidazolium ionic liquid (IL). This catalyst promoted the Huisgen 1, 3-dipolar cycloaddition of organic azides and terminal alkynes efficiently. At the end of reaction, the catalyst is easily separated by an external magnet, without using extra organic solvents and additional filtration steps and reused without loss of catalytic activity or leaching of copper species.

Experimental

Reagents and analysis

Chemical materials were purchased from Merck and Aldrich Chemical Companies in high purity. All the solvents were distilled, dried and purified by standard procedures.

Melting points were measured on an Electrothermal 9100 apparatus. The samples were analyzed using fourier transform infrared (FT-IR) spectroscopy (ABB-Bomem MB-100 in KBr matrix). The X-ray powder diffraction (XRD) of the catalyst was carried out on a Philips PW 1830 X-ray diffractometer with $\text{CuK}\alpha$ source ($\lambda=1.5418 \text{ \AA}$) in a range of Bragg's angle ($10\text{-}80^\circ$) at room temperature. Scanning electron microscope (SEM) pictures-EDS analyses were taken using VEGA//TESCAN KYKY-EM3200 microscope (acceleration voltage 26 kV). Transmission electron microscopy (TEM) experiments were conducted on a Philips EM 208 electron microscope. ^1H , ^{13}C NMR spectra were recorded on a BRUKER DRX-400 AVANCE spectrometer. Mass spectra were recorded on a FINNIGAN-MATT 8430 mass spectrometer operating at an ionization potential of 20 eV. Elemental analyses for C, H and N were performed using a Heraeus CHN-O-Rapid analyzer. Thermo gravimetric analysis (TGA) was recorded on a Stanton Redcraft STA-780 (London, UK). Magnetic measurements were performed using vibration sample magnetometry (VSM, MDK, and Model 7400) analysis. A simultaneous ICP-OES (Varian Vista-Pro, Springvale, Australia) coupled to a V-groove nebulizer and equipped with a charge-coupled device (CCD) was applied for determination of the trace metal ions.

General procedure

Synthesis of vinyl functionalized magnetic nanoparticles (MNPs@MPS)

An iron salt solution was obtained by mixing $\text{FeCl}_3 \cdot 6\text{H}_2\text{O}$ (2.35 g, 8.7 mmol) and $\text{FeCl}_2 \cdot 4\text{H}_2\text{O}$ (0.86 g, 4.3 mmol) in deionized water (40 mL). The resultant solution was left to stir for 30 min at 80°C . Then NH_3 (25%, 5 mL) of was added with vigorous stirring to produce a black precipitate and the reaction was continued for another 30 min. The precipitate, was isolated by magnetic decantation, washed several times with deionized water and then dried at 80°C for 10

h. Dried Fe_3O_4 nanoparticles (0.5 g) were suspended in a solution of ethanol (50 mL) and NH_3 (25%, 5 mL). Then, tetraethoxysilane (TEOS, 0.2 mL) was added dropwise to the above suspension, and the mixture was ultrasonicated for two h. Afterward silica coated Fe_3O_4 (MNPs) was magnetically separated, washed three times with ethanol and dried at 80°C for 10 h. MNPs (100 mg) was dispersed in dry ethanol (15 mL) by ultrasonication and then NH_4OH solution (0.2 mL) was added into the flask. Next, an excess amount of 3-(trimethoxysilyl) propylmethacrylate (MPS) (4 mL) was added dropwise and the mixture was stirred at 60°C for 48 h. The MPS coated magnetic nanoparticles (MNPs@MPS) were magnetically separated and washed several times with ethanol and dried under at 50°C for 12 h [23].

Synthesis of [VIM-COOH][Cl] monomer and cross-linker BVD

Chloroacetic acid (2.82 g, 30 mmol) was dissolved in toluene (300 mL), and 1-vinylimidazole (2.82 g, 30 mmol) was added to the solution and the mixture was refluxed for 24 h. Then, the reaction mixture was cooled to room temperature, and the liquid was poured out, and the solid was washed three times by acetonitrile (20 mL) to remove the unreacted starting materials. After drying in a vacuum for 24 h, a light yellow solid was obtained as IL monomer [VIM-COOH][Cl] (5.1 g, 90% yield).

For preparation of 1,4-butane-diyl-3,3'-bis-1-vinylimidazolium dibromide (BVD) as cross-linking agent, 1-vinylimidazole (2.82 g, 30 mmol) and 1,4-dibromobutane (13 g, 60 mmol) were stirred in methanol at 60°C for 20 h. The reaction mixture was then cooled to room temperature and added to diethyl ether (250 mL). The resulting translucent solution was placed in a refrigerator for 5 h. Solid products were separated by decantation of supernatant and washed three times with diethyl ether and dried under vacuum at 50°C for 12 [24a].

Synthesis of catalyst (MNP@ImAc/Cu)

MNP@MPS (0.5 g), [VIM-COOH][Cl] (1 g) and BVD (0.4 g) were loaded into a 100 mL round bottom flask and methanol (40 mL) was added. The mixture was sonicated for 20 min and then deoxygenated under argon for another 20 min. Afterwards, AIBN (5 mg) was added to the mixture and the flask was equipped with a condenser and placed in an oil bath at 70 °C. After 24 h, the solid products were magnetically separated and washed three times with methanol and dried under vacuum at 60 °C. For neutralization of carboxylic acid groups within the polymer network, powdered magnetic solid was dispersed in water (25 mL), and an excess amount of K₂CO₃ solution was added, and the mixture was stirred for 20 h in room temperature. The obtained solid MNP@ImAc was magnetically separated and washed with water for three times and dried in vacuum at 60 °C for 12h.

The obtained MNP@ImAc (0.5 g) was dispersed in deionized water at room temperature and an aqueous solution of copper sulfate (1M, 25 mL) was added to the mixture and mixture was stirred for 24 h at 50 °C. The resulting solid was magnetically separated and washed five times with water (5×20 mL) and dried under vacuum to give MNP@ImAc/Cu for 12h.

Determination of the copper content in MNP@ImAc/Cu

The MNP@ImAc/Cu (100 mg) was extracted with concentrated HCl (5 × 2 mL) in a screw-capped vessel, followed by treatment with concentrated nitric acid (2 mL) to digest the metal complex. The mixture was then transferred into a volumetric flask (100 mL), diluted 1:50 for the second time and was analyzed by the inductively coupled plasma-optical emission spectrometry (ICP-OES) analysis [24b]. The loading of copper ion on the supported catalyst was calculated to be 13.23 wt % (2.1 mmol g⁻¹).

General procedure for synthesis of 1,4-disubstituted triazoles

Primary halides (1 mmol), NaN₃ (1.2 mmol, 0.08 g) and terminal alkynes (1 mmol) were placed in a 10 mL round-bottom flask in H₂O (3 mL). Sequentially, MNP@ImAc/Cu (1 mg, 0.2 mol %) and sodium ascorbic (10 mol%, 0.02 g) was added to solution. The reaction mixture was stirred at room temperature and the completion of reaction was monitored by TLC. After completion of the reaction, the catalyst was magnetically separated and washed several times with EtOH followed by water and dried under vacuum for 12h. The residue was extracted with EtOAc (2×10 mL) followed by drying with anhydrous Na₂SO₄. After evaporation of the solvent, the desired pure product was isolated in the case, if necessary the product was further purified by recrystallized by EtOAc-hexane mixtures or EtOH. The products were characterized with IR, ¹HNMR and ¹³CNMR spectroscopies.

The retreatment of the recovered catalyst

After several cycles, when the reaction rates were reduced, the recovered catalyst in the click reaction, was retreated with copper sulfate solution. For this purpose, recovered catalyst (0.05 gr) was stirred in aqueous solution of copper sulfate (0.1 M, 10 mL) at 50 °C for 6 h. The brown residue was separated by an external magnet and washed with water several times. The catalyst was dried for 24 h and reused in the next reaction (Table 8, Regenerated catalyst).

Results and discussion

Fabrication of the catalyst

The synthesis of MNP@ImAc/Cu is shown in Fig. 1. Initially, Co-precipitation of FeCl₃ and FeCl₂ in an ammonia solution led to formation of Fe₃O₄ nanoparticles (MNPs). Then a layer of SiO₂ was coated on Fe₃O₄ surface to improve the chemical stability and biocompatibility of particles. Afterward, the surface of MNP was modified by MPS (MNPs@MPS) to ensure that MNPs covalently bonded to the copolymer chains. Copolymerization was initiated by AIBN and

in the presence of BVD as a cross-linker. During the polymerization magnetic nanoparticles were entrapped into the cross-linked polymer matrix and covalently attached to polymer chains. By this method, a multi-layered form of polymer is formed and enveloped the magnetic nanoparticles. After preparation of solid support, carboxylic acid groups are neutralized by base. Then, copper sulfate was loaded onto the support surface through the strong coordination with numerous carboxylate groups.

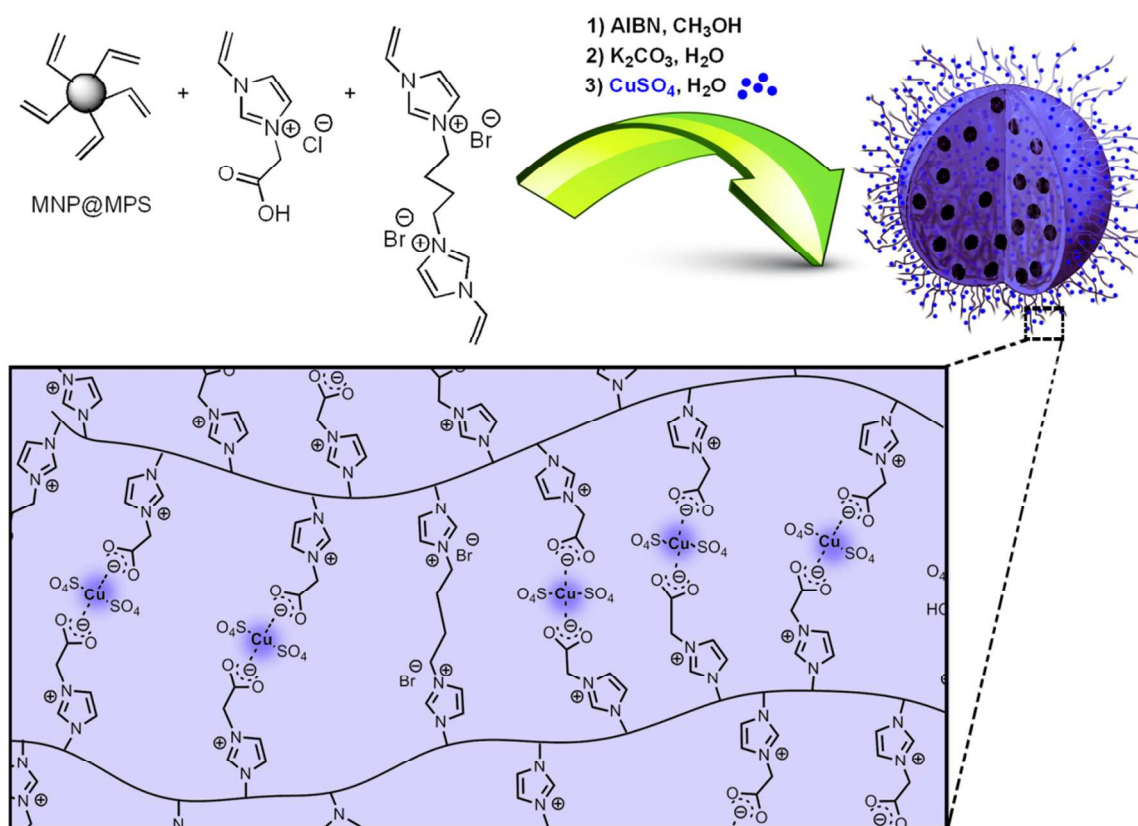


Fig. 1. Synthesis of MNP@ImAc/Cu catalyst

Despite conventional immobilization of ionic liquids on the support surface which usually leads to low loading of immobilized ionic liquid, in this method, the solid support is made by ionic

liquid monomer, which improves the loading level of supported catalyst. Actually, in this method magnetic nanoparticles are coated by several layers of polymer chains, and a magnetic composite is formed. The resulting support has numerous coordination sites, which can adsorb a large number of copper ions and increases the loading level of copper on the support surface.

The fourier transform infrared spectra (FTIR) identifies chemical bonds in the prepared samples. Fig. 2 shows FTIR of bare MNPs (b), MNP@MPS (c), MNP@ImAc (d) and MNP@ImAc/Cu (e). In the FTIR spectrum of MNPs (Fig. 1a), the characteristic adsorption band of Fe-O is observed at 624 cm^{-1} . The broad band at $3300\text{--}3500$ is due to -OH stretching vibrations. The presence of the characteristic peak of Si-O at 1062 cm^{-1} confirms the formation of the silica shell of around the Fe_3O_4 core. The characterization peaks of MNP are observed in all spectra, confirming the existence of MNPs in all samples. The FT-IR spectrum of MNP@MPS (Fig. 1b) shows strong stretching vibration bands of carbonyl groups (1714 cm^{-1}), C=C (1610 cm^{-1}) and C-H (2923 cm^{-1}) indicate that MPS was successfully attached to the surface of MNPs. Fig. 1c shows the FT-IR spectrum of MNP@ImAc with characteristic peaks in 1561 cm^{-1} , 1630 cm^{-1} , 1740 cm^{-1} , attributed to C-N, C=N and C=O stretching vibrations of the imidazole rings and -COOH groups, respectively. This result shows that solid magnetic support MNP@ImAc was successfully prepared. In the spectrum of MNP@ImAc/Cu (Fig. 1d), all characteristic peaks of MNP@ImAc is observed. Moreover, the stretching vibration band of S=O is observed at 1133 cm^{-1} , indicating that CuSO_4 is successfully immobilized on the support surface.

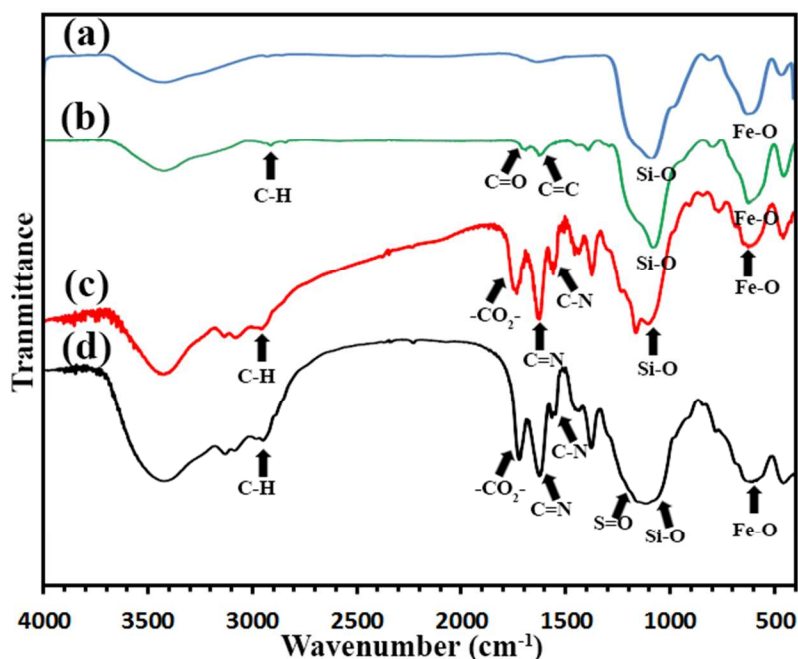


Fig. 2. FTIR spectra of (a) bare MNPs, (b) MNP@MPS, (c) MNP@ImAc and (d) MNP@ImAc/Cu.

The results of elemental analysis of MNP@MPS, MNP@ImAc and MNP@ImAc/Cu are tabulated in Table 1. Comparison between CHNS analysis of MNP@MPS and MNP@ImAc shows that the content of C, H and N atoms increased in MNP@ImAc, indicating MNP@MPS was successfully coated by polymer chains. Increasing in sulphur content in MNP@ImAc/Cu is attributed to immobilize CuSO_4 .

Table 1. Elemental analysis for catalyst

Samples	C%	H%	N%	S%
MNP@MPS	6.15	1.45	-	-
MNP@ImAc	25.32	3.54	8.61	-
MNP@ImAc/Cu	24.13	3.66	8.02	16.40
Recycled MNP@ImAc/Cu	25.76	3.92	7.87	4.63

Thermogravimetric analysis (TGA) and derivative thermogravimetric (DTG) were performed in the range of 25 to 800 °C, to determine the loading of organic groups coated onto the surface of the magnetite. Fig. 3 shows the TGA and DTG of MNP (a), MNP@MPS (b) and MNP@ImAc/Cu (c). In all samples, weight loss within 100–200 °C is due to the physically adsorbed water molecules and hydroxyl groups at the magnetite surface. MNPs@MPS shows 10% weight loss at 250–600 °C corresponding to the thermal decomposition of the grafted propylmethacrylate groups onto the MNPs surface. From this weight loss, the loading amount of MPS onto the MNP surface was calculated 0.78 mmol/g. After polymerization, the weight loss in MNP@ImAc/Cu increased again which was due to thermal degradation of polymeric content. Based on TG analysis, MNP@ImAc/Cu exhibited good thermal stability under 300 °C. The TGA pattern for MNP@ImAc/Cu (Fig. 3) shows the drastic weight loss of nearly 44% at 250–500 °C for the cross-linked polymeric network.

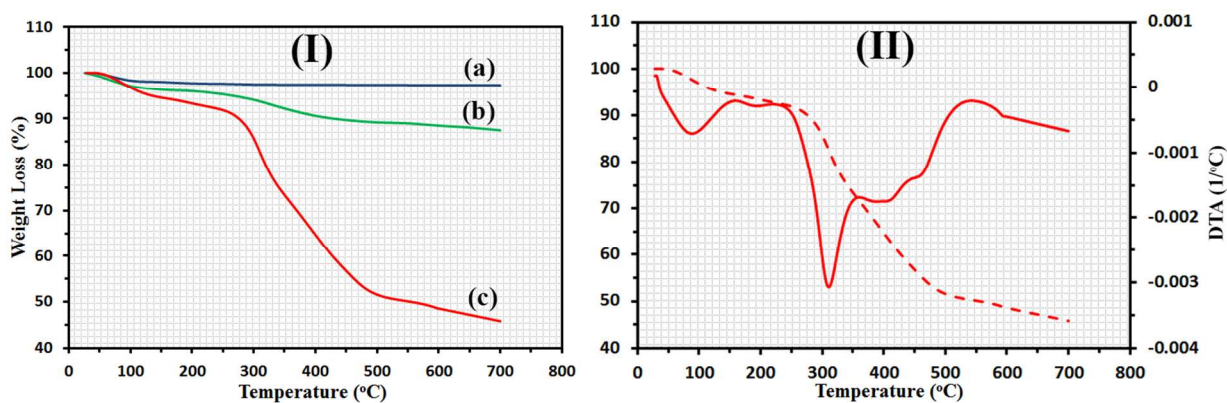


Fig. 3. (I): (a) TGA of MNP, (b) MNP@MPS and (c) MNP@ImAc/Cu; (II) DTG of MNP@ImAc/Cu.

The average particles' size and morphology of nanoparticles were investigated by scanning electron microscopy (SEM) and transmission electron microscopy (TEM). Fig. 4 presents the TEM images of MNP (a) and MNP@ImAc/Cu (b). From the TEM image of MNP the size of the sphere magnetic nanoparticles is around 7-15 nm. As shown in the TEM image of MNP@ImAc/Cu, magnetic nanoparticles are embedded into the polymeric matrix.

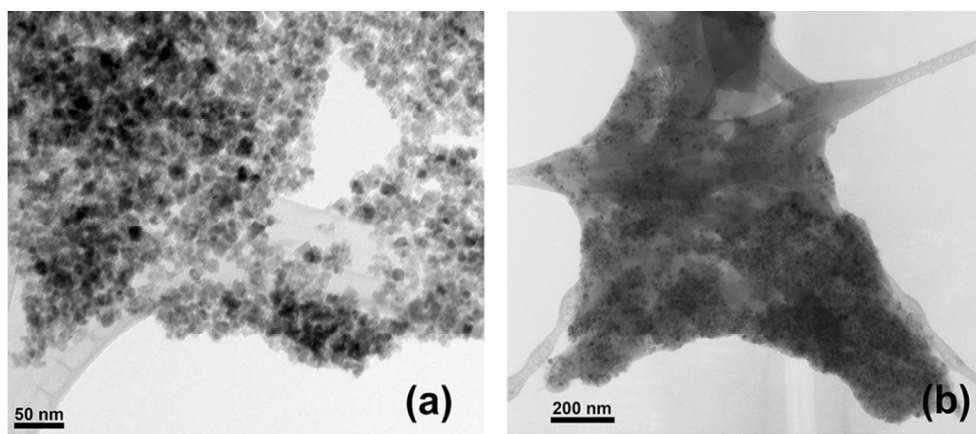


Fig. 4. TEM images of (a) MNP and (b) MNP@ImAc/Cu

The scanning electron microscopy (SEM) image of MNP@ImAc/Cu (Fig. 5) shows that the surface of catalyst is rough due to the presence of MNPs. This rough morphology of catalyst surface may improve the catalytic activity by increasing the available catalytic site. The energy dispersive X-ray spectroscopy (EDAX) analysis of MNP@ImAc/Cu (Fig. 5) confirms the presence of copper and iron in catalyst structure.

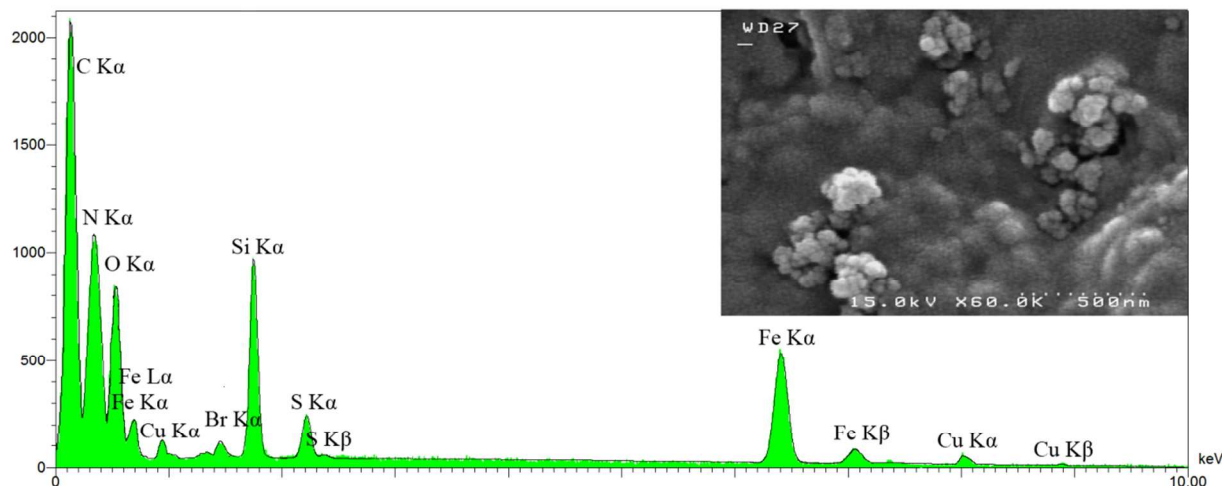


Fig. 5. SEM image and EDAX analysis of MNP@ImAc/Cu

The magnetic properties of MNP (a) and MNP@ImAc/Cu (b) were determined by a vibration sample magnetometer (VSM), and magnetic hysteresis curves are shown in Fig. 6. The VSM curve for MNP@ImAc/Cu shows that its saturation magnetization value was 29 emu/g without the observation of hysteresis curves, indicating the typical superparamagnetic behavior. The saturation magnetization of MNP@ImAc/Cu is smaller than that of bare MNPs due to entrapment of MNPs into the nonmagnetic materials. However, the magnetization is still large enough for separation of the catalyst.

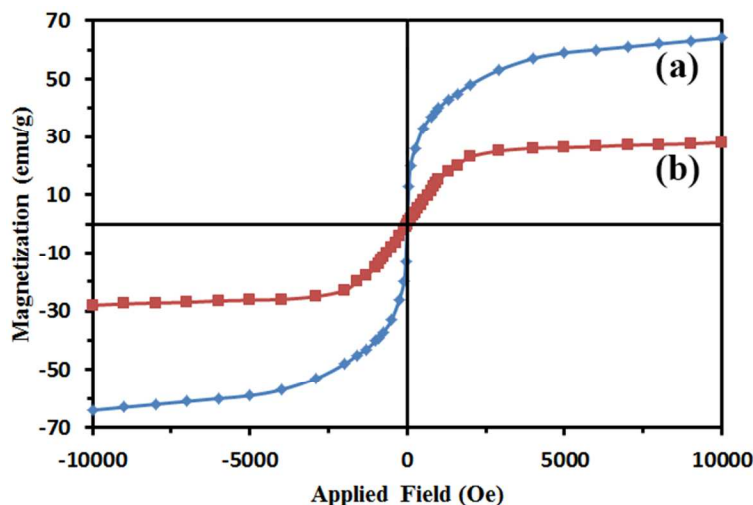


Fig. 6. VSM curves of (a) MNP and (b) MNP@ImAc/Cu

The crystalline structures of prepared nanoparticles were analyzed by X-ray powder diffraction (XRD). The XRD pattern of MNPs (Fig. 7b), shows peaks at 2θ values 30.1° , 35.4° , 43.1° , 53.4° , 57° and 62.6° related to (220), (311), (400), (422), (511) and (440) crystal planes in Fe_3O_4 cubic lattice, which agrees well with the standard structure of Fe_3O_4 (JCPDS card no. 85-1436). The XRD pattern of MNP@ImAc/Cu (Fig. 7a) contains the above peaks together with a broad peak from 20° to 30° that could be assigned to the synergetic effect of amorphous silica.

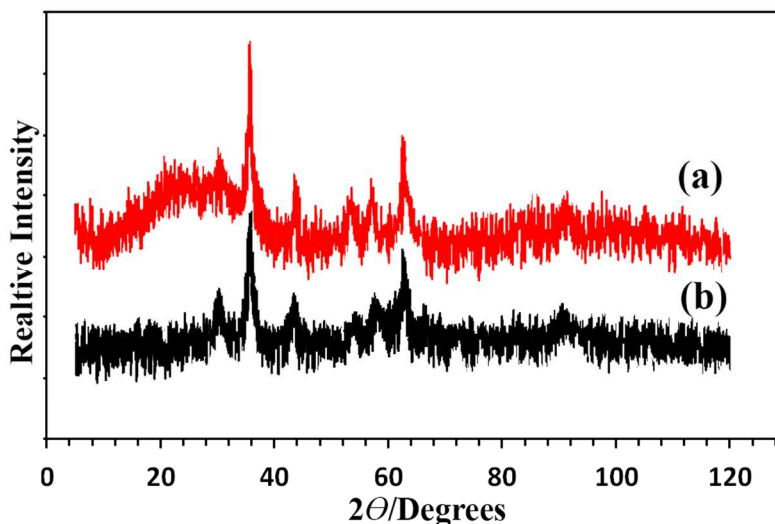


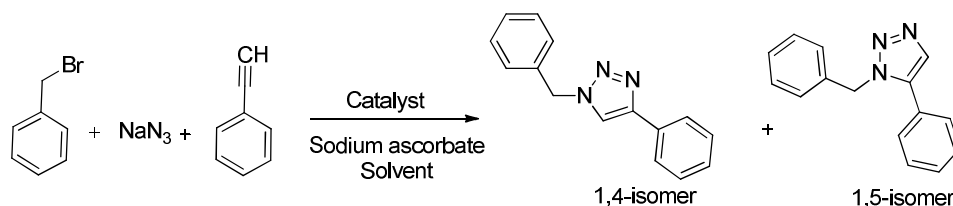
Fig.7. XRD patterns of (a) MNP@ImAc/Cu and (b) MNP.

All the data discussed above confirms that the magnetic nanoparticles are embedded into the polyvinylimidazolium chains and a magnetic composite with a large number of copper ions is formed.

Catalytic Performance of MNP@ImAc/Cu

The catalytic activity of MNP@ImAc/Cu was tested in the multicomponent 1, 3-dipolar cycloaddition reaction of terminal alkynes, sodium azide and alkyl halides or tosylates, along with 10 mol% of sodium ascorbate. The reaction of phenylacetylene (1 mmol) benzyl bromide (1 mmol), NaN_3 (1.2 mmol) and sodium ascorbate (10 mol%) was chosen as a model reaction and the reaction was examined in different conditions, and the results are presented in Table 2. It can be seen that when the model reaction was carried out at room temperature in the aqueous medium in the absence of any catalyst, no desired product was formed after 5 h (entry 1). Also, no significant product was observed with bare MNP or MNP@ImAc as the catalyst in water after 5 h (entries 2 and 5). On the other hand, CuSO_4 and $\text{CuSO}_4/\text{ImAc}$ as the homogeneous catalysts resulted in 15% and 65% yields in water in 5 h (entries 3 and 4). But using 3 mg MNP@ImAc as the catalyst gave 99% yield in 1h. Reducing the amounts of catalyst demonstrates that 1 mg MNP@ImAc is enough for completion of the reaction (entries 6-9). Different solvents and solvent/co-solvent mixtures were tested, and water was found to be the most effective medium for this reaction (entries 8 and 10-14). Increasing the reaction temperature to 70 °C reduced the reaction time to 30 min for completion of reaction. Absence of sodium ascorbate as a reducing agent of Cu II to Cu I, clearly demonstrates the effect of sodium ascorbate in this reaction (Entry 17). The model reaction was also carried out in the presence of MNP@IMAcCu(I) under the same reaction conditions, and the desired product was formed in 75% yield after 2h (entry 18). This is in agreement of the observations reported in the literature that the catalytic active Cu(I)

species directly generated by reduction with ascorbate, immediately forms Cu-acetylides, but CuCl salts require high temperature to form the Cu-acetylide complexes [24c]. The results show that the highest yield of 1-benzyl-4-phenyl-1H-1,2,3-triazole was achieved with 1 mg catalyst in water for only 1 h at room temperature (Entry 8). On the other hand, it is interesting to note that under this condition, no other byproducts were observed.

Table 2. Optimization of the reaction conditions for synthesis of 1,4-disubstituted 1,2,3 triazoles

Entry ^a	Catalyst	Cat. Loading (Cu mol%)	Solvent	<i>T</i>	Time	Yield (%) ^b
1	-	-	H ₂ O	r.t	5 h	-
2	MNP	3 mg	H ₂ O	r.t	5 h	trace ^c
3	CuSO ₄	0.6	H ₂ O	r.t	5 h	15
4	CuSO ₄ /ImAc	0.6	H ₂ O	r.t	5 h	65
5	MNP@ImAc	3 mg	H ₂ O	r.t	5 h	-
6	MNP@ImAc/Cu	3 mg, 0.6	H ₂ O	r.t	1 h	99
7	MNP@ImAc/Cu	0.4	H ₂ O	r.t	1 h	99
8	MNP@ImAc/Cu	0.2	H ₂ O	r.t	1 h	99
9	MNP@ImAc/Cu	0.1	H ₂ O	r.t	1 h	82
10	MNP@ImAc/Cu	0.2	H ₂ O: EtOH	r.t	1 h	91
11	MNP@ImAc/Cu	0.2	EtOH	r.t	1 h	30
12	MNP@ImAc/Cu	0.2	THF	r.t	1 h	trace
13	MNP@ImAc/Cu	0.2	MeOH	r.t	1 h	65
14	MNP@ImAc/Cu	0.2	Hexane	r.t	1 h	55
15	MNP@ImAc/Cu	0.2	H ₂ O	50 °C	1 h	99
16	MNP@ImAc/Cu	0.2	H ₂ O	70 °C	0.5 h	99
17	MNP@ImAc/Cu	0.2	H ₂ O	r.t	1 h	trace ^d
18	MNP@ImAc/Cu(I) ^e	0.2	H ₂ O	r.t	2 h	78

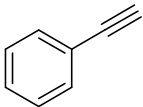
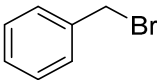
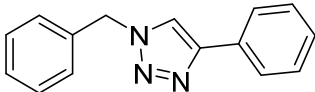
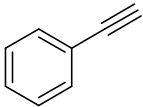
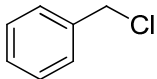
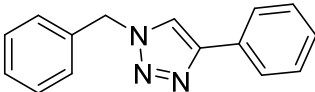
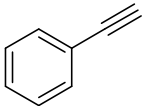
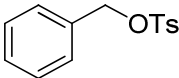
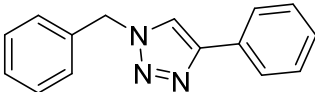
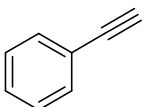
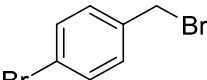
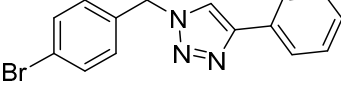
^a All of reaction were carried out under conditions: benzyl bromide (1 mmol, 0.12 mL), NaN₃ (1.2 mmol, 0.08 g), phenyl acetylene (1 mmol, 0.10 mL), solvent (3 mL) and sodium ascorbate (10 mol%, 0.02 g). ^b Isolated yield. ^c mixture of 1,4- and 1,5- isomers, ^d Without using of sodium ascorbate, ^e MNP@ImAc/Cu(I) was prepared from MNP@ImAc and CuCl in H₂O.

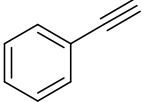
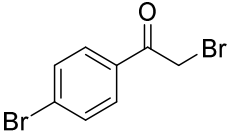
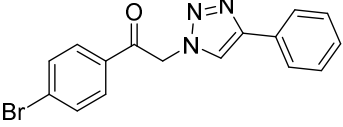
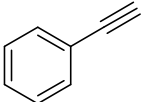
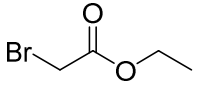
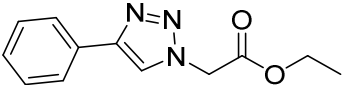
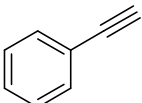
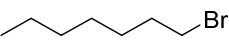
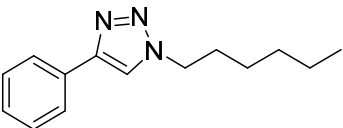
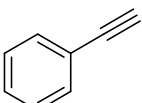
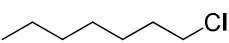
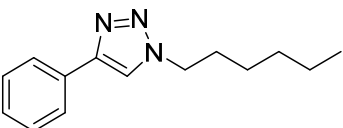
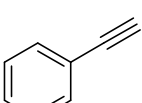
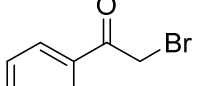
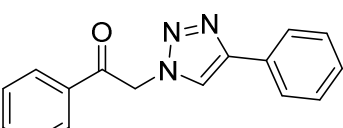
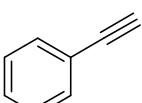
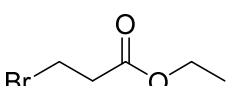
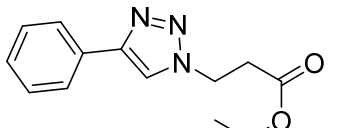
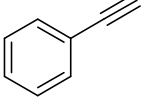
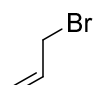
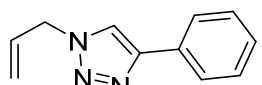
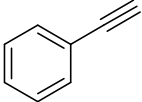
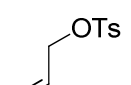
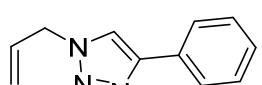
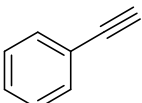
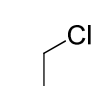
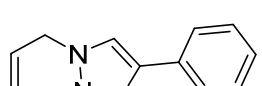
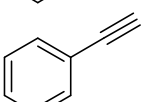
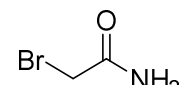
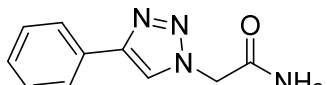
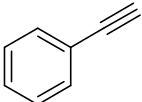
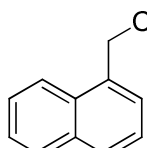
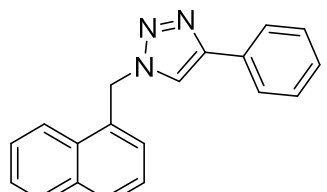
In order to explore the generality and applicability of this catalyst, a variety of primary halides or tosylates with alkynes and NaN₃ were reacted under the optimal reaction conditions and the results are summarized in Table 3. In all cases, the transformation provided regiospecifically the 1,4-substituted 1,2,3-triazoles in satisfactory to excellent yields. Different benzyl bromides

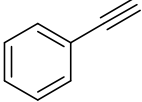
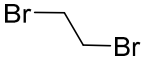
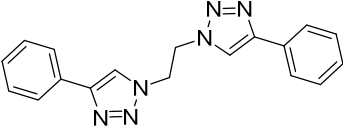
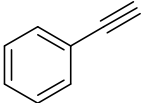
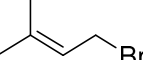
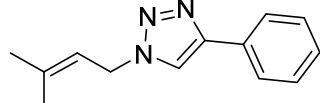
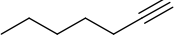
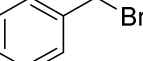
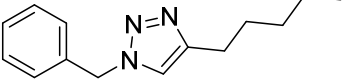
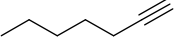
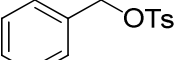
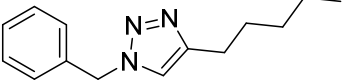
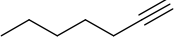
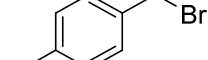
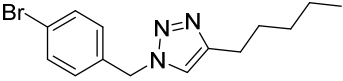
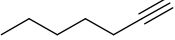
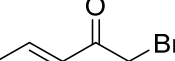
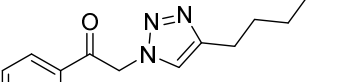
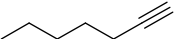
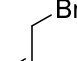
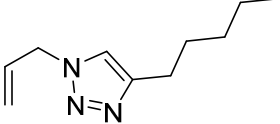
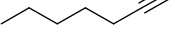
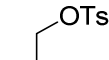
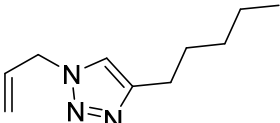
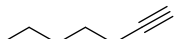
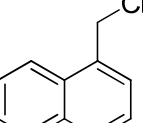
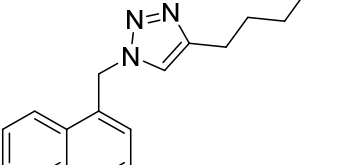
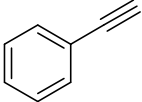

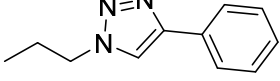
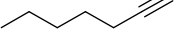

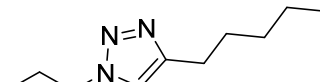
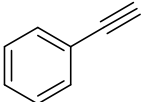

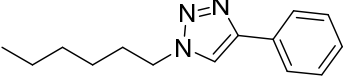
reacted well with alkynes and NaN_3 to afford the corresponding triazoles in nearly quantitative yields. In the case of activated functionalized organic halides such as *p*-bromo phenacyl bromide, phenacyl bromide, ethyl bromoacetate and acetamide bromide, the reactions proceeded smoothly and the products were isolated in high yields. Allyl bromide reacted as well as its benzyl counterpart. As it is clear, aliphatic alkyl bromides tolerated well in this reaction. It was found that terminal dibromoalkane (1,2-dibromoethane) reacts with 2 equal of phenylacetylene to give bistriazole product. Aliphatic alkynes, such as 1-heptyne also gave the expected triazoles in good to high yields, although in longer reaction times compared with their aryl counterparts.

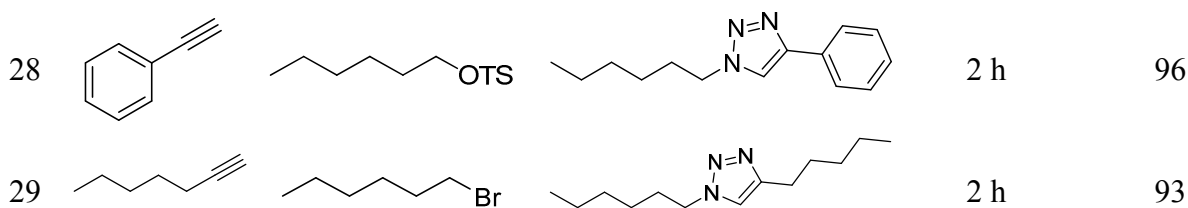
To investigate the practical applicability of the catalyst in scale up reaction, the model reaction was repeated in 20 mmol scale under similar optimized reaction condition. The reaction was proceeds well with 91% isolated yield in 1h.

Table 3. Huisgen 1,3-Dipolar Cycloaddition Catalyzed by MNP@ImAc/Cu^a

Entry	Alkyne	Alkyl/Aryl halide	Product	Time	Yield (%) ^b
1				1 h	99
2				2 h	93
3				1 h	99
4				1 h	97

5				3 h	91
6				3 h	90
7				3 h	93
8				5 h	98
9				3 h	92
10				2 h	94
11				2 h	96
12				1 h	99
13				3 h	97
14				2 h	89
15				5 h	88

16				5 h	91
17				1 h	90
18				3 h	91
19				3 h	95
20				3 h	97
21				3 h	91
22				3 h	92
23				3 h	90
24				4 h	82
25				2 h	94
26				2 h	94
27				2 h	93



^a Reaction condition: alkyne (1 mmol), primary halide or tosylate (1mmol), NaN₃ (1.2 mmol, 0.08 g), sodium ascorbate (10 mol%, 0.02 g), MNP@ImAc/Cu (1 mg, 0.2 mol%), H₂O (3 mL), r.t., ^b Isolated yield.

Reuse test of MNP@ImAc/Cu

For a heterogeneous catalyst, it is essential to study its ease of separation, recoverability and recyclability. The reusability of MNP@ImAc/Cu was investigated in the synthesis of 1,4-substituted 1,2,3-triazole by choosing the reaction between benzylbromide, phenyl acetylene and sodium azide under the optimized reaction condition. After completion of the reaction, catalyst was easily removed using a magnet and recovered by washing with EtOH, and vacuum drying. The recovered catalyst was reused for ten times without a significant decrease in catalytic activity (Fig 8). However, after fifth run a longer reaction time was needed for completion of the reaction which is due to the mass loss of catalyst during the separation and washing the catalyst. Therefore, by losing the mass of catalyst more time was needed for completion of the reaction. After several cycles, when the reaction rates were reduced, the recovered catalyst was retreated, and the thus regenerated catalyst resumed the initial activity of the fresh one, showing conversion of 99% for 60 min. This demonstrates a good regenerate capability for MNP@ImAc/Cu (Table 8, Regenerated catalyst).

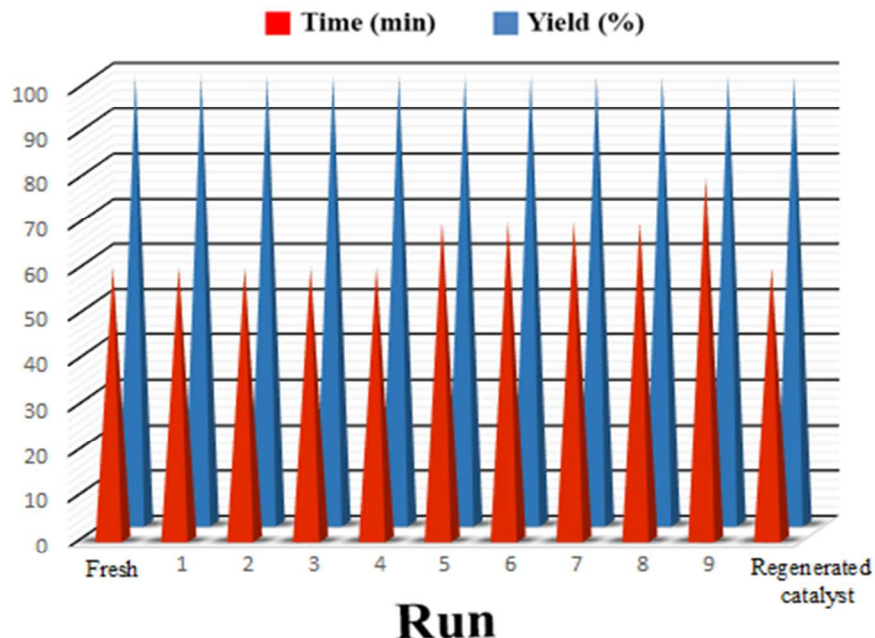


Fig. 8. Recyclability of MNP@ImAc/Cu

To explore the catalyst leaching, the reaction between benzylbromide, phenyl acetylene and sodium azide was carried out under optimized condition. After 30 min (half of needed time for completion of reaction) the reaction was stopped and the catalyst was magnetically separated. The yield of product was measured by GC (68%). The residue was then allowed to react without catalyst for another 90 min. After that, the reaction mixture was analyzed by GC and the result showed that no significant conversion was observed after catalyst separation (Fig. 9). Also, the amount of loaded metal onto the surface was also measured by inductively coupled plasma-optical emission spectrometry (ICP-OES). The result of ICP-OES analysis for the reaction mixture and product showed no copper species. The results of CHNS analysis after catalyst recycling showed no significant change in C, H and N contents. However, after recycling sulfur atom content is reduced due to the exchange of SO_4^{2-} anions with ascorbate (Table 1). The content of copper in the reused catalyst was analyzed by ICP-OES, and the result showed no

significant change in copper loading (13.12 wt%, 2.08 mmol/g copper). The TEM image of catalyst after recycling shows no change in catalyst structure (Fig. S1). These results show that MNP@ImAc/Cu is highly stable, and the catalyst is truly heterogeneous. Moreover, we have found that no special handling precaution regarding exposure to air/moisture needs to be taken in the use of MNP@ImAc/Cu as the catalyst.

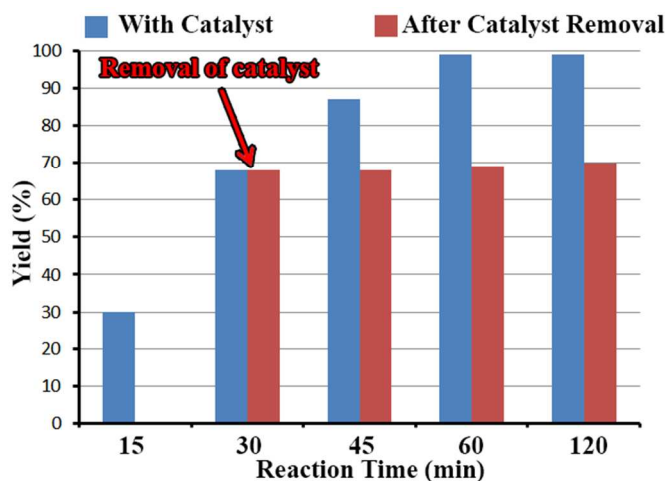


Fig. 9. Catalyst leaching experiment

Comparison with other reported systems

Performances of MNP@ImAc/Cu and previously reported catalysts were compared in Table 4.

Although, all the methods are effective, but the present procedure comparatively affords a truly green process with high yield of the products in shorter reaction time at room temperature, and carries out these reactions in water using magnetically separable nanoparticles as the catalyst.

It is worth noting that the loading amount of copper ion in MNP@ImAc/Cu is relatively high.

This property of catalyst is especially useful in large-scale application where the amount of expensive catalyst should be low.

Table 4. The comparison of MNP@ImAc/Cu with reported catalysts in the synthesis of triazoles

Catalyst	Copper Loading on Catalyst (mmol/g)	Catalyst Loading (mol%)	Time	<i>T</i>	Yield (%)	Ref
Functionalized Chitosan/Cu	0.6	0.1	12 h	70 °C	99	[25]
Cross-linked polymeric ionic liquid/Cu	1.0	1.0	48 h	r.t	98	[26]
Ionic Polymer /Cu	0.25	5	2.5 h	r.t	99	[27]
Poly(4-vinyl pyridine)/Cu	1.32	13	0.4 h	100 °C	89	[28]
Nano ferrite-glutathione-copper	0.25	2.5	0.17 h	120 °C, mw ^c	99	[7]
Poly(NIPAM/Im)/Cu	0.46	0.25	1.5 h	50 °C	99	[29]
Poly(NIPAM/Im)/Cu	0.46	0.00045	31 h	50 °C	94	[29]
MNP-CuBr	0.44	1.46	0.3 h	80 °C, mw ^c	96	[21]
Cu/Al ₂ O ₃	0.29	10	1 h	r.t.	92	[9]
Cu(II)/Clay	1.5	2	0.25 h	sonic.r.t	98	[10]
Cu/SiO ₂	2.59	10	0.17 h	70 °C or 50 °C, mw ^c	92	[30]
CuNPs/MagSilica	1.07	4.3	1 h	70 °C	98	[30]
Cu NP/Activated carbon	0.25	0.5	3 h	70 °C	98	[31]
MNP@ImAc/Cu	2.1	0.2	1 h	r.t.	99	- ^b

^a Click reaction of benzybromide, sodium azide, and phenylacetylene, ^b Present work, ^c microwave system

Conclusion

A novel copper magnetic catalyst based on poly(ionic liquid) was synthesized and showed to be a highly efficient heterogeneous catalyst for one-pot synthesis of 1,4-disubstituted 1,2,3-triazoles in water at room temperature without using any toxic solvent or co-catalyst. This protocol is clean and safe process and can be used to generate a diverse range of products in good to excellent yields. Because of the polymeric nature of coating material, loading amount, recyclability and catalytic activity of catalyst is largely promoted. Moreover, this nanocatalyst is stable showing no aggregation and copper leaching and can be recycled many times without loss of catalytic activity. From the viewpoint of green chemistry, the present protocol was proven to be useful and has been potential for use in industrial applications.

References

1. A. S. Matlack, *Introduction to Green Chemistry*, Marcel Dekker, New York, 2001.
2. H. Shintaku, K. Nakajima, M. Kitano, N. Ichikuni, M. Hara, *ACS Catal.* 2014, **4**, 1198–1204.
3. S. A. Bakunov, S. M. Bakunova, T. Wenzler, M. Ghebru, K. A. Werbovets, R. Brun, R. R. Tidwell, *J. Med. Chem.*, 2010, **53**, 254-272.
4. R. Alvarez, S. Velazquez, F. San, S. Aquaro, C. De, C.F. Perno, A. Karlsson, J. Balzarini, M. J. Camarasa, *J. Med. Chem.*, 1994, **37**, 4185-4194.
5. R. Huisgen, *In 1,3-Dipolar Cycloaddition Chemistry*; Padwa, A., Ed.; Wiley: New York, 1984.
6. a) V. V. Rostovtsev, L. G. Green, V. V. Forkin, K. B. Sharpless, *Angew. Chem., Int. Ed.*, 2002, **41**, 2596-2599. b) C. W. Tornøe, C. Christensen, M. Meldal, *J. Org. Chem.* 2002, **67**, 3057-3064.
7. R. B. Nasir Baig, R. S. Varma, *Green Chem.*, 2012, **14**, 625-632, b) B. Dervaux, F. E. Du Prez, *Chem.Science*, 2012, **3**, 959-966., c) A. Megia-Fernandez, M. Ortega-Muñoz, J. Lopez-Jaramillo, F. Hernandez-Mateo, F. Santoyo-Gonzalez, *Adv. Synth. Catal.* 2010, **352**, 3306 -3320.
8. B. S. P. Anil Kumar, K. H. V. Reddy, B. Madhav, K. Ramesh, Y. V. D. Nageswar, *Tetrahedron Lett.*, 2012, **53**, 4595–4599.
9. N. Mukherjee, S. Ahammed, S. Bhadra, B. C. Ranu, *Green Chem.*, 2013, **15**, 389-397.
10. B. A. Dar, A. A. Bhowmik, A. Sharma, P.R. Sharma, A. Lazar, A. P. Singh, M. Sharma, B. Singh, *Appl. Clay Sci.*, 2013, **80 – 81**, 351 –357.
11. A. Coelho, P. Diz, O. Caamaço, E. Sotelo, *Adv. Synth. Catal.*, 2010, **352**, 1179-1192.

12. Y. Monguchi, K. Nozaki, T. Maejima, Y. Shimoda, Y. Sawama, Y. Kitamura, Y. Kitade, H. Sajiki, *Green Chem.*, 2013, **15**, 490 – 495.
13. M. Nasr-Esfahani, I. Mohammadpoor-Baltork, A. R. Khosropour, M. Moghadam, V. Mirkhani, S. Tangestaninejad, H. A. Rudbari, *J. Org. Chem.* 2014, **79**, 1437-1443.
14. I. Jlalía, F. Gallier, N. Brodie-Linder, J. Uziel, J. Augé, N. Lubin-Germain, *J. Mol. Catal. A*, 2014, **393**, 56-61.
15. Y. Kitamura, K. Taniguchi, T. Maegawa, Y. Monguchi, Y. Kitade, H. Sajiki, *Heterocycles*, 2014, **88**, 233-243.
16. L. Wan, C. Cai, *Catal. Lett.* 2012, **142**, 1134–1140.
17. I. Luz, F.X. Llabrés, I. Xamena, A. Corma, *J. Catal.* 2010, **276**, 134-140.
18. B. Dervaux, F. E. Du Prez, *Chem. Sci.*, 2012, **3**, 959-966.
19. J. Safari, Z. Zarnegar *C. R. Chimie*, 2013, 821–828.
20. F. Nador, M. A. Volpe, F. Alonso, A. Feldhoff, A. Kirschning, G. Radivo, *Appl. Catal., A* 2013, **455**, 39-45.
21. X. Xiong, L. Cai, *Catal. Sci. Technol.*, 2013, **3**, 1301-1307.
22. P. Veerakumar, M. Velayudham, K. Lu, S. Rajagopal, *Catal. Sci. Technol.*, 2011, **1**, 1512–1525.
23. A. Pourjavadi, S. H. Hosseini, F. Matloubi Moghaddam, B. K. Foroushani, C. Bennett, *Green Chem.*, 2013, **15**, 2913-2919.
24. (a) J. Yuan, M. Antonietti, *Macromolecules*, 2011, **44**, 744 –750, (b) J. A. Albadi, M. Keshavarz, M. Abedini, M. Khoshakhlagh, *J. Chem. Sci.*, 2013, **125**, 295–298. (c) M. Melda, C. W. Tornøe, *Chem. Rev.* 2008, **108**, 2952–3015.
25. M. Chtchigrovsky, A. Primo, P. Gonzalez, K. Molvinger, M. Robitzer, F. Quignard, F. Taran, *Angew. Chem.*, 2009, **121**, 6030-6034.

26. Y. Wang, J. Liu, C. Xia, *Adv. Synth. Catal.*, 2011, **353**, 1534-1542.
27. U. Sirion, Y.J. Bae, B. S. Lee, D. Y. Chi, *Synlett*, 2008, **15**, 2326-2330.
28. J. Albadi, M. Keshavarz, F. Shirini, M. Vafaie-nezhad, *Catal. Commun.*, 2012, **27**, 17–20.
29. Y. M. A. Yamada, S. M. Sarkar, Y. Uozumi, *J. Am. Chem. Soc.*, 2012, **134**, 9285-9290.
30. C. S. Radatz, L. d. A. Soares, E. f. R. Vieira, D. Alves, D. Russowsky, P. H. Schneider, *New J. Chem.*, 2014, **38**, 1410-1417.
31. F. Alonso, Y. Moglie, G. Radivoy, M. Yus, *Adv. Synth. Catal.*, 2010, **352**, 3208 – 3214